Design and Synthesis of Biomimetic Multicomponent All-Bone-Minerals Bionanocomposites

Abhijit Biswas,*,† Ilker S. Bayer,*,§ He Zhao,†,‡ Tao Wang,† Fumiya Watanabe,|| and Alexandru S. Biris*,||

Center for Nanoscience and Technology (NDnano), Department of Electrical Engineering and Department of Aerospace and Mechanical Engineering, University of Notre Dame, Notre Dame, Indiana 46556, United States, Italian Institute of Technology, Smart Materials Group, Arnesano, LE 73010, Italy, and Nanotechnology Center, University of Arkansas at Little Rock, Little Rock, Arkansas 72204, United States

Received August 10, 2010; Revised Manuscript Received September 12, 2010

We report a simple and novel top-down method based on a drop-casting process for the controlled synthesis of all-bone-minerals biomimetic multicomponent bionanocomposites. Integration of micro- and nanoscale binary features into nanofibrous biocompatible polymer scaffold structures is successfully demonstrated. Compositional control of the constituents of the bionanocomposites resulted in uniform dispersion of hydroxyapatite nanospheres (∼100−500 nm) among collagen nanofibers (∼100 nm). The composites also present high calcium and oxygen contents and adequate phosphorus compositions comparable to the levels of bone tissues. Our preliminary results open up further possibilities to develop advanced tissue-engineered bionanocomposites for bone grafting.

1. Introduction

Bone is a specialized form of connective tissue that forms the skeleton of the body and is built on the nano and micro levels as a multicomponent composite material consisting of a hard inorganic phase (minerals) in an elastic, dense organic network. The key bone minerals and chemical elements are hydroxylapatit, also called hydroxyapatite (HAP), collagen protein fibers, phosphorus, and calcium. The combination of inorganic and organic phases not only provides bone with unique mechanical properties and a reservoir for minerals such as calcium and phosphate but also serves as a medium for diffusion and release of biological substances.[1−9]

Despite the fact that bone is the mechanically strongest tissue in the body and has the capability of self-regenerating, it often can undergo major biological and mechanical damages or defects caused by a number of diseases or injuries. Bone grafting is commonly employed to treat such bone defects. The key functions of bone grafts are to provide mechanical or structural support, fill defective gaps, and enhance bone tissue formation while providing a scaffold for bone cellular proliferation. The ultimate goal of bone grafting is the restoration of healthy bone tissue to reduce the volume of the bone defects generated due to trauma or biological processes. The conventional procedure for bone grafting is to procure bone tissues from the healthy donor, process, and reimplant them at the locations where the bone replacement or reconstruction is required. However, such a natural grafting process has limitations due to several factors such as the possibility of pathogen transfer, graft rejection, patient additional trauma, limited available bone tissue, and so on.[1,10]

Whereas implantable, porous blocks may be prepared with varying degrees of porosity as artificial bone materials,[11] a number of drawbacks limit their applications. Block scaffolds do not generally have therapeutic agents embedded throughout the implanted device. Also, implantable blocks are not injectable and thus require a more invasive surgical procedure. Furthermore, monolithic blocks may impede the rate of bone formation for clinical applications where an acceleration of healing is desired. Other materials such as cements are readily injectable and can have the therapeutic substances embedded throughout the volume of the device. However, cements have the tendency to form monolithic aggregates with relatively poor porosity, which encourages channeling rather than widespread diffusion throughout the device. This behavior significantly restricts new bone growth.[12] To circumvent these problems, new artificial biocompatible and bone-mimicking materials need to be developed that can be employed for bone grafting or implantation purposes with limited risk of rejection and infections.

Bionanocomposites are promising new artificial bone materials that use a combination of several biocompatible materials and bone minerals and structurally tuned to resemble the natural bone structure.[9,13] They are derived from natural and synthetic biodegradable polymers such as polysaccharides, aliphatic polyesters, polypeptides, proteins, and polynucleic acids and organic/inorganic fillers such as clays, HAP, and metal nanoparticles.[14] Biocompatible organic matrix provides required mechanical strength and flexibility to the minerals including HAP and collagen fibers. These nanocomposites offer larger surface area, high surface reactivity, relatively strong interfacial bonding, and better design flexibility compared with conventional bulk composites.[1,9,13] Additionally, they offer the possibility of creating bone grafts using bone tissue engineering processes that involve the effective applications of bone or stem cells, scaffolding and cell−scaffold interactions.

It is highly desired that bionanocomposites are suitably designed and synthesized having all of the important bone minerals that are grown in intimate contact with a biocompatible organic matrix rich in collagen fibers. An ideal biomimetic or

* To whom correspondence should be addressed. E-mail: abiswas@nd.edu (Abhijit Biswas); ilker.bayer@gmail.com (Ilker Bayer); asbiris@ualr.edu (Alexandru Biris).
† Center for Nanoscience and Technology (NDnano), Department of Electrical Engineering, University of Notre Dame.
‡ Department of Aerospace and Mechanical Engineering, University of Notre Dame.
§ Italian Institute of Technology.
|| University of Arkansas at Little Rock.

10.1021/bm1009359
Published on Web 09/23/2010

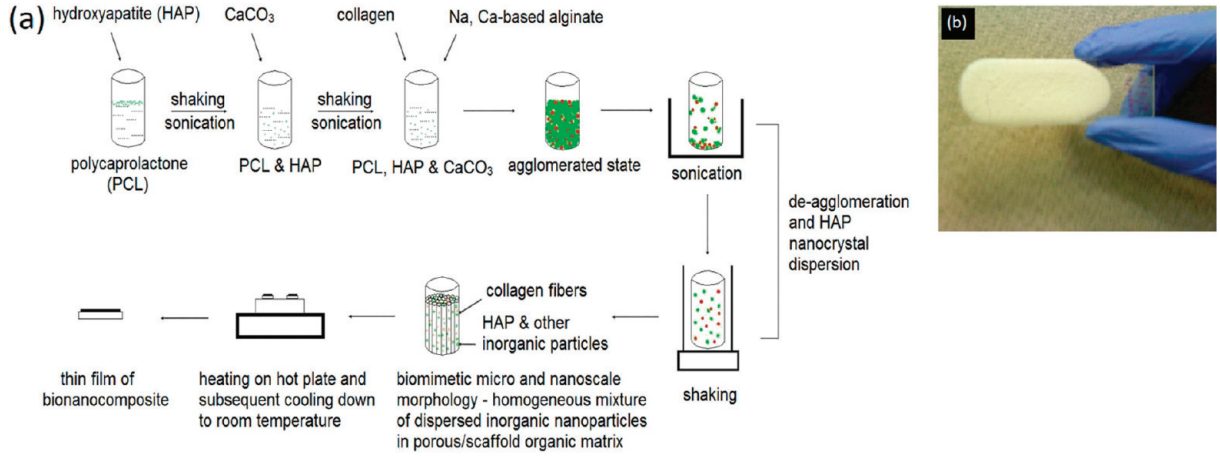

Figure 1. (a) Schematic illustration of the synthesis process of bionanocomposite. (b) Photograph of the bionanocomposite bone material (length: 2.1 in; width: 1 in; thickness: 5 mm) on a glass slide after heat curing.

bone-mimetic bionanocomposite would replicate the predominant coalignment of the organic and mineral phase. This essentially involves nano- to macroscale features of both the organization of collagen fibers in a characteristic 3D architecture and the coalignment of important mineral such as HAP crystals within the collagen fibers. It is a significant challenge from the materials synthesis point of view to achieve such complex and special 3D multicomponent bone-like features. Another consideration for a suitable design of bionanocomposites is to employ calcium-rich bone minerals along with adequate phosphorus to maintain the required bone mineral density (BMD), which is required for the treatment of metabolic bone diseases such as osteoporosis (thinning of the bone matrix) and osteomalacia (softening of the bone and decreased bone density).[15] Furthermore, one of the major problems in the current state-of-the-art implants is the low oxygen supply, which causes poor bone cell proliferation.[16,17] The cells of bone receive oxygen from limited sources (the nutrient artery being the major one). Hence, it is very important that the bionanocomposite materials have sufficiently high elemental oxygen available that can help maintain revascularization for nutrient and compensate for the loss of oxygen delivered to cells.

As mentioned before, it is challenging to synthesize such multicomponent materials with homogeneous mixing of several components because of the fact that the interfacial adhesion among several ingredients might fail during the growth process, causing the formation of cracks and mechanical defects over time. Among other reported approaches, the prominent ones are the bottom-up biomimetic routes that have been shown to produce bionanocomposites with HAP crystals in a bioactive polymer/collagen.[1,13,18] Biomimetic approaches follow self-assembly of biochemical processes of molecules that involve a complex bottom-up route, which may not be highly efficient to combine and grow several bone minerals simultaneously in a fibrous protein-rich biocompatible matrix together with desired required structure.

In this Communication, we report a simple top-down synthesis process based on a drop-cast method to synthesize multicomponent bionanocomposites consisting of homogeneous mixture of all bone minerals. This low-cost and simple approach can be applied for large scale synthesis of artificial bone materials. The method allows the preparation of complex and multicomponent bone-like materials with the desired bone-mimetic features just by applying the required compositional and processing parameters. It enables us to achieve the important nano- to macroscale bone-mimetic features, including the organization of collagen nanofibers in a characteristic 3D architecture that is typical of the bone tissue and the coalignment of HAP nanospheres within the collagen nanofibers.

We show successful incorporation and uniform mixing of several bone minerals such as HAP, $CaCO_3$, collagen, sodium, and calcium-based polysaccharide or alginate (alginic acid salt from brown algae) and citrate in a polycaprolactone (PCL) matrix. The tailoring of the structure resulted in collagen-rich nanofibrous matrix, which is highly desired for tissue regeneration. Uniform dispersion of porous HAP spheres with a diameter range between 100 and 500 nm embedded in nanofibers of collagen was achieved. An elemental compositional scheme resulted in high calcium and oxygen contents of the bionanocomposites. We achieved significant structural control over the integration of the required 3D scaffold structures, generating high porosity by combining micro- and nanoscale features that are required to match the natural bone structures.

2. Experimental Section

Figure 1 schematically illustrates the dropcast synthesis route (a) and a photograph of bionanocomposite film after curing (b). Initially, ~120 mg PCL pellets (molecular weight: 14 000; Sigma-Aldrich) were added to 20 mL of benzyl alcohol (Alfa-Aesar) in a 100 mL beaker. Under room temperature, a transparent homogeneous PCL solution was generated using sonication and mechanical shaking. About 100 mg of HAP nanopowder (Sigma-Aldrich, size <200 nm) was then added to the prepared homogeneous PCL solution. This was followed by sonication and extensive mechanical shaking, which resulted in a homogeneous solution of PCL and HAP. Following this, ~50 mg of $CaCO_3$ nanopowder (Specialty Minerals, Ultra-Pflex, size ~70 nm) along with minimal ingredients of calcium-based alginate powders (Sigma-Aldrich) were added. Finally, 5 mL of collagen in liquid state (Invitrogen, collagen 1, bovine for cell culture) was mixed together with the composite solution. Samples were prepared on glass slides and petridish for further analyses and studies. The gel-state bionanocomposite sample on glass slide was first heated to 50 °C on a hot plate for ~10 min. It was then cooled to room temperature to form a thin film.

In the applied method, the parameters to control the bionanocomposite growth process are essentially of a compositional nature. For example, the amounts of $CaCO_3$ and HAP were varied to obtain relatively higher oxygen and calcium along with adequate phosphorus content in the bionanocomposites. A weight ratio of 90 mg/60 mg between HAP and $CaCO_3$ was applied to obtain higher calcium and

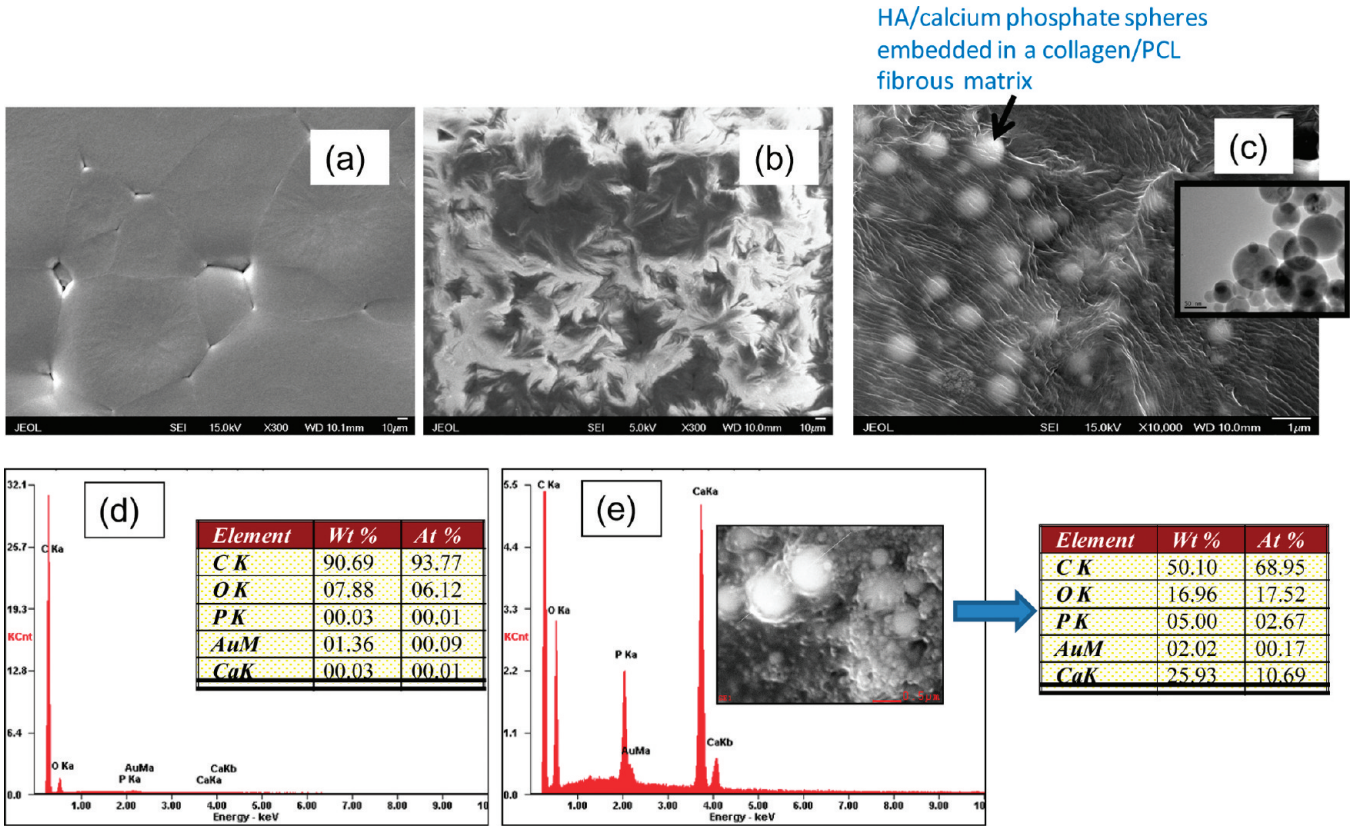

Figure 2. SEM overview images of (a) polymer (PCL) gel and (b) scaffold/porous structures of bionanocomposite consists of polycaprolactone (PCL), hydroxyapatite (HAP), calcium carbonate ($CaCO_3$), collagen, calcium, and sodium-based alginate. (c) Higher magnified SEM image of HAP spheres embedded in collagen-rich fibrous matrix. The inset of part c shows a TEM image of the HAP nanopowder used in this work. Energy dispersive X-ray (EDX) analysis of (d) PCL and (e) EDX line scan of HAP spheres and the matrix along with the corresponding elemental compositions that are shown in the Table. EDX measurements show an oxygen-rich bionanocomposite system. The Au signal is due to the coating of a thin layer of Au over the surface of the samples.

oxygen. Also, processing conditions such as sonication and shaking time, growth temperature, and gradual mixing of bone minerals were carefully controlled to achieve the desired structural morphology.

3. Results and Discussion

Figure 2 shows the scanning electron microscope (SEM) images of (a) pristine polymer (PCL) sample and (b,c) scaffold/porous structure of bionanocomposite and a higher resolution image of the bionanocomposite morphology respectively. Figure 2d,e shows corresponding SEM EDX data of polymer and the line scan of HA spheres. The SEM microscope used for analysis was a JEOL 7000 FE (resolution 1.2 nm at 30 KV) coupled to an EDX system for elemental analysis. Our transmission electron microscope (TEM) analysis of the HAP nanopowder (Sigma-Aldrich) used in this work showed spherical HAP nanocrystals (<200 nm) (Figure 2c, inset).

A scaffold with a highly porous morphology and hydrophilic surface is extremely important for bone tissue engineering by using biodegradable and biomimetic material scaffolds integrated with biological cells or molecules.[10] Furthermore, computational modeling predicted that integration of micro- and nanoscale features into designed scaffolds could improve both mechanical properties through toughening mechanisms and tissue regeneration through improved control of cell adhesion.[10] Moreover, such an arrangement would mimic the actual bone tissue architecture, which is formed by both nano- and microstructures.

We achieved morphological and structural control required to produce these important features. Figure 2b,c shows porous matrix structures along with the combination of micro- and nanoscale binary features within the scaffolds. These bionanocomposites have hierarchical surface roughness as well as micro- and nanosized pores. Advanced SEM image analysis indicates a large fraction of the composite morphology comprises micro/nanopores. Macro (micro) pore size distribution was found to range between 10 and 50 μm. In general, there seems to be a good degree of connectivity between the pores. However, some big pores around 50 μm do not seem to form complete holes or pores within the composite from top to bottom surface. These pores tend to terminate with smaller 1−5 μm puncture-like holes or pores toward the bottom of the biofilm. This is actually a quite unique feature because it can still allow material transport properties across the bionanocomposite film. Smaller micro pores with the size of ~10 μm seem to go quite deep into the composite film. Furthermore, around the inorganic nanoparticle fillers the pores are on the order of 200 nm with a significantly narrower distribution. These pores seem to concentrate around the edges of the HAP nanofillers or nanofiller agglomerates.

Figure 2c shows the HAP spheres of size of about 100−500 nm embedded with the nanofibers (~100 nm) of collagen. Previous study has shown that fiber formation results in substantial stabilization of collagen.[19] Fiber-like structures usually do not form in the case of thermally induced collagen degradation, suggesting a thermal stability of collagen in the synthesized bionanocomposites cured at 50 °C. Figure 2c shows collagen nanofibers organized parallel to each other, which is a crucial morphological arrangement for enhanced mechanical

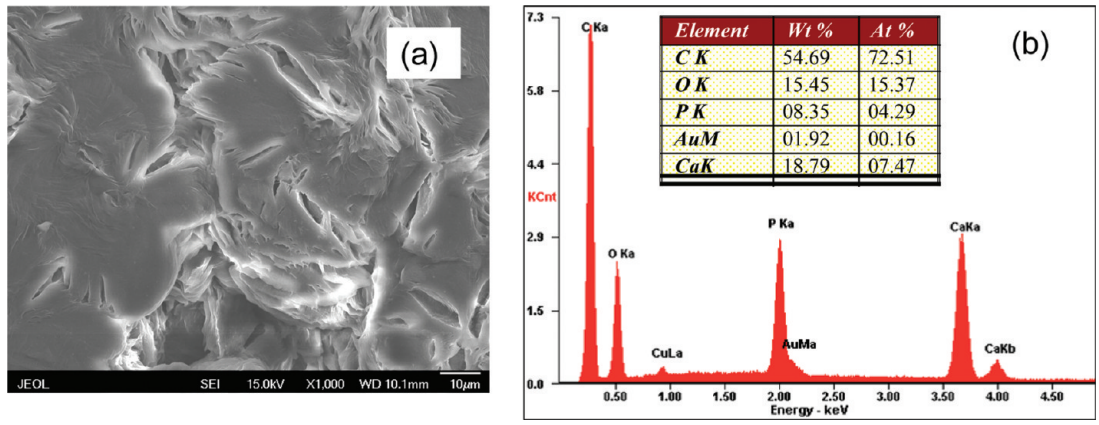

Figure 3. (a) Typical overview SEM image of a bionanocomposite with higher HAP concentration. (b) SEM EDX analysis shows the corresponding elemental composition. The Au signal is due to the coating of nanocomposites by Au, whereas the Cu signal comes from the SEM grid.

properties and which is normally found in healthy bone tissues.[20,21] Note that these uniformly distributed nanofibers along with the architecture and organization were generated using a simple inexpensive dropcast method. The existing current techniques to produce such nanofibrous scaffolds for tissue engineering include relatively complex processes such as electrospinning, self-assembly, and phase separation.[22]

Spherical HAP granules are desired because they were possibly shown to eliminate or limit the nondesirable inflammation reactions of the body. The rounded granules with smooth geometry (Figure 2c) are preferable for a variety of medical applications such as tissue-engineered bone graft, bone cement, targeted delivery of protein, peptide, and macromolecules.[23−25]

The EDX data in Figure 2d,e show elemental compositions of the pure polymer and bionanocomposites. The EDX scan of the polymer (PCL) (Figure 2d) indicates the residual-trace presence of Ca and P that might be due to minor experimental cross contamination during materials preparation or measurements. The bionanocomposites show high oxygen and calcium contents at 17 and 26 wt %, respectively (Figure 2e). A biomaterial rich with calcium along with adequate supply of phosphorus is highly required for the treatment of metabolic bone diseases. Furthermore, as previously described, oxygen-rich bionanocomposites would be ideal for bone cell growth.[15−17] The presence of oxygen-containing groups onto the surface of the nanocomposites was previously shown to increase cellular proliferation due to the increased hydrophilicity and optimum surface energy.[26]

To investigate the structural morphology and elemental composition of bionanocomposites with much higher HAP concentrations, we increased the concentration of HAP while keeping the same concentration of $CaCO_3$ as that in the previous case. The SEM results indicated a more uniform mixing of HAP granules and their arrangements within the bulk. A better mixing implies that the HAP minerals will be dispersed completely within the polymer matrix. Figure 3 shows an overview SEM image of a bionanocomposite with higher HAP concentration along with the corresponding EDX data showing the elemental compositional profile.

Increasing HAP concentration in the bionanocomposites clearly altered the elemental compositions of phosphorus, calcium, and oxygen, as indicated by the EDX data (Figure 3b). It is apparent that higher HAP concentrations are responsible for higher phosphorus contents. Figure 2b indicates that the ratio of atomic percentages of calcium to phosphorus is approximately 2:1, which is considered to be ideal for maintaining a healthy BMD.[27,28] Further investigations regarding cell culture and animal studies over the multicomponent bionanocomposites are in progress in our laboratory.

4. Conclusions

We have presented a simple top-down method based on a dropcast synthesis process for controlled synthesis of bionanocomposites comprising all-bone-minerals. We have achieved important structural control, allowing us to generate 3D nanofibrous scaffold structures with HAP nanospheres (∼100−500 nm) embedded in collagen nanofibers (∼100 nm). This shows successful integration of micro- and nanoscale features into biocompatible polymer scaffolds, which is required for developing advanced biomimetic and biocompatible materials for bone grafting using tissue engineering. The synthesized bionanocomposites have high calcium, oxygen, and adequate phosphorus contents needed to maintain healthy levels of BMD and bone cell growth. Our preliminary results open up further possibilities to develop advanced artificial biomaterials for the treatment of bone disease.

Acknowledgment. The authors from Notre Dame gratefully acknowledge financial support from the Center for Nanoscience and Technology (NDnano) at the University of Notre Dame. H.Z. acknowledges Nanoelectronics Undergraduate Research Fellowship (NURF) provided by NDnano.

References and Notes

(1) Murugan, R.; Ramakrishna, S. *Compos. Sci. Technol.* **2005**, *65*, 2385–2406.
(2) Seto, J.; Gupta, H. S.; Zaslansky, P.; Wagner, H. D.; Fratzl, P. *Adv. Funct. Mater.* **2008**, *18*, 1905–1911.
(3) Fratzl, P.; Weinkamer, R. *Prog. Mater. Sci.* **2007**, *52*, 1263–1334.
(4) Chappard, C.; Marchadier, A.; Benhamou, C. *Bone.* **2008**, *43*, 203–208.
(5) Weiner, S.; Wagner, H. D. *Annu. Rev. Mater. Sci.* **1998**, *28*, 271–298.
(6) Giraud-Guille, M. M. *Calcif. Tissue Int.* **1988**, *42*, 167–180.
(7) Traub, W.; Arad, T.; Weiner, S. *Proc. Natl. Acad. Sci. U.S.A.* **1989**, *86*, 9822–9826.
(8) Glimcher, M. J. *Rev. Mineral. Geochem.* **2006**, *64*, 223–282.
(9) Hule, R. A.; Pochan, D. J. *MRS Bull.* **2007**, *32*, 354–358.
(10) Hollister, S. J. *Nature* **2005**, *4*, 518–524.
(11) Liu, Y. L.; Schoenaers, J.; Groot, K. de.; Wijn, J. R.; de; Schepers, E. *J. Mater. Sci.: Mater. Med.* **2000**, *11*, 711–717.
(12) Huber, F.-X.; Belyaev, O.; Hillmeier, J.; Kock, H.-J.; Huber, C.; Meeder, P.-J.; Berger, I. *BMC Musculoskeletal Disord.* **2006**, *7*, 50.

(13) Darder, M.; Aranda, P.; Ruiz-Hitzky, E. *Adv. Mater.* **2007**, *19*, 1309–1319.
(14) Yamaguchi, I.; Tokuchi, K.; Fukuzaki, H.; Koyama, Y.; Takakuda, K.; Monma, H.; Tanaka, J. J. *Biomed. Mater. Res.* **2001**, *55*, 20–27.
(15) Kaufman, J. M. *Clin. Rheumatol.* **1995**, *14*, 9–13.
(16) Ross Garett, I.; Boyce, F. B.; Oreffo, O. C. R.; Bonewald, L.; Poser, J.; Mundy, R. G. *J. Clin. Invest.* **1990**, *85*, 632–639.
(17) Kloss, F. R.; Francis, L. A.; Sternschulte, H.; Klauser, F.; Gassner, R.; Rasse, M.; Bertel, E.; Lechleitner, T.; Steinmüller-Nethl, D. *Biomaterials* **2008**, *29*, 2433–2442.
(18) Ruiz-Hitzky, E.; Darder, M.; Aranda, P.; Ariga, K. *Adv. Mater.* **2009**, *22*, 323–336.
(19) Privalov, P. L. *Adv. Protein Chem.* **1982**, *35*, 1–104.
(20) Ruppel, M. E.; Miller, L. M.; Burr, D. B. *Osteoporos Int.* **2008**, *19*, 1251–1265.
(21) Nassif, N.; Gobeaux, F.; Seto, J.; Belamie, E.; Davidson, P.; Panine, P.; Mosser, G.; Fratzl, P.; Giraud-Guille, M. M. *Chem. Mater.* **2010**, *22*, 3307–3309.
(22) Smith, I. O.; Liu, X. H.; Smith, L. A.; Ma, P. X. *Wiley Interdiscip. Rev.: Nanomed. Nanobiotechnol.* **2009**, *1*, 226–236.
(23) Paul, W.; Sharma, S. T. *J. Mater. Sci.: Mater. Med.* **1999**, *10*, 383–388.
(24) Komlev, V. S.; Barinov, S. M.; Koplik, E. V. *Biomaterials,* **2002**, *23*, 3449–3454.
(25) Scachschal, S.; Pich, A.; Adler, H.-J. *Colloid Polym. Sci.* **2007**, *285*, 1175–1180.
(26) De, S.; Sharma, R.; Trigwell, S.; Laska, B.; Ali, N.; Mazumder, M. K.; Mehta, J. L. *J. Biomater. Sci., Polym. Ed.* **2005**, *16*, 973–989.
(27) Teegarden, D.; Lyle, R. M.; McCabe, G. P.; McCabe, L. D.; Proulx, W. R.; Michon, K.; Knight, A. P.; Johnston, C. C.; Weaver, C. M. *Am. J. Clin. Nutr.* **1998**, *68*, 749–754.
(28) Tzaphlidou, M.; Zaichick, V. *Biol. Trace Elem. Res.* **2003**, *93*, 63–74.

BM1009359